PHYSICAL REVIEW A **73**, 022719 (2006)

Excitation of atoms and molecules by highly relativistic ions

M. Bär, B. Jakob, P. -G. Reinhard, and C. Toepffer
Institut für Theoretische Physik II, Universität Erlangen–Nürnberg, Staudtstrasse 7, D–91058 Erlangen, Germany

(Received 24 November 2005; published 24 February 2006)

We study the cross section for inelastic collisions of atoms and small molecules under the influence of highly relativistic charged ions as they occur in storage rings and accelerators. Starting from fully time-resolved calculations of the electronic dynamics, we study a set of complementing approximations, a sudden approximation for the extremely fast collision at low impact parameter combined with time-dependent perturbation theory for the weak and slow collisions at large impact parameters. This leads eventually to a simple, yet reliable, estimate in terms of the ion-hydrogen cross section and the variance of the dipole moment for the actual system. We discuss, in particular, the systems H, He, C, N, O, Ne, H_2, and N_2.

DOI: 10.1103/PhysRevA.73.022719 PACS number(s): 34.10.+x, 31.70.Hq, 34.50.Fa

I. INTRODUCTION

Collisions of charged energetic projectiles with atoms or molecules are a generic process that has been studied under a great variety of conditions and circumstances; for a detailed overview, see Ref. [1]. Robust estimates in terms of scaling laws for the ionization cross sections have been developed as early as 1930 [2] and have been refined further later on [3,4]. Steadily increasing numerical and experimental techniques have triggered a widespread literature on that subject in its various facettes. There are, for example, several experimental and theoretical studies of *K*-shell ionization [5–8] and more general excitations [9] in relativistic ion-atom collisions. The theoretical estimates in these publications employ predominantly perturbation theory. Fully fledged numerical calculations of collisional ionization are presented, e.g., in Refs. [10–13]. The present paper discusses from a theoretical perspective the excitation of atoms and small molecules through highly relativistic ions. The aim is to develop an efficient description based on microscopic calculations leading to compact estimates. The motivation comes from the physics of storage rings for high-energy particles [14,15]. The goal is to estimate the cross section for inelastic collisions of the stored ions with atoms or molecules from the residual gas. Such collisions have two aspects: on the one hand, they are an unwanted perturbation of the stored beam, and on the other hand, one may take advantage of those events to gather useful information about the beam and the state of the vacuum from the subsequent radiative decay of the excited residual gas [16]. In any case, one needs reliable theoretical estimates for the inelastic collision cross sections. It is the aim of this paper to provide the cross sections for a variety of atoms and dimer molecules as they are typical for the rest gases.

Starting point and benchmark are a time-dependent description of the target electrons by time-dependent density-functional theory (TDDFT) [17] where the by-passing ion is acting just as a source for a fast electromagnetic pulse. Fully time-resolved calculations grow extremely expensive because pulses from highly relativistic ions have a time scale that is orders of magnitude shorter than the periods of the target electrons. We thus invoke a sudden approximation along the lines of the Glauber approximation in scattering theory [18,19] similarly as it was used previously in Ref. [20]. The sudden approximation applies to near collisions with their extremely short time scales. We check against the fully time-resolved calculations. Distant collisions, on the other hand, produce broad, but weak, pulses. That case is tractable by perturbation theory. We thus work with different approximations for the various regimes and we take care to connect them properly. This yields finally a rather inexpensive estimate for the cross section which requires some input from the presently easily available DFT calculations.

II. FORMAL FRAMEWORK

A. The setup

The scattering process is followed in an explicit time-dependent picture. The fast ion is described as a Coulomb charge propagating along a classical trajectory. The perturbation by the target atom is extremely small. We thus assume that the ion passes by on a straight trajectory,

$$\mathbf{R}_{\text{ion}}(t) = (b, 0, \beta ct), \quad \beta = \frac{v}{c} \tag{1}$$

characterized by the velocity $\beta = v/c$ and the impact parameter b. It moves parallel to the z axis. On the same footing, we neglect the recoil of the target. The center of the target (atom or molecule) is placed at the origin of the coordinate system. The target nuclei are frozen in space. Only its electron cloud is considered as a dynamical degree of freedom. The cloud is described in terms of time-dependent single-electron wave functions $\{\varphi_\alpha, \alpha = 1, \ldots, N\}$ through the time-dependent density functional theory (TDDFT) [17]. It reduces to the time-dependent Schrödinger equation in the case of the simple hydrogen atom.

B. The external field

The excitation is mediated by the external Coulomb field of the fast ion. Its Coulomb and vector potentials read

$$\Phi = -\frac{\gamma Z e}{\sqrt{(x-b)^2 + y^2 + d^2 + \gamma^2 (z - \beta ct)^2}}, \tag{2a}$$

$$\gamma = \frac{1}{\sqrt{1-\beta^2}}, \tag{2b}$$

and $A_x=0$, $A_y=0$, $A_z=\beta\Phi$. The expression contains the small parameter d which serves to cut off the Coulomb singularity at the position of the ion. It is introduced for practical reasons. For the electrons of the target system, we are going to solve the Kohn-Sham equations on a grid in coordinate space which requires such a cutoff typically of the order of the grid spacing. We chose it small enough to make the results independent of the cutoff.

The potentials (2) have the great disadvantage to decay very slowly, namely $\propto r^{-1}$ (where $r=\sqrt{x^2+y^2+z^2}$). The physical forces in terms of electrical and magnetic fields fall off much faster. We bring the potentials into a more convenient shape by the gauge transformation $\Phi \rightarrow \Phi + (1/c)\partial_t\Lambda$, $\mathbf{A} \rightarrow \mathbf{A} + \boldsymbol{\nabla}\Lambda$, $\varphi \rightarrow \exp(\imath\Lambda)\varphi$, with

$$\Lambda = \frac{1}{\beta}\mathrm{Ar\,sinh}\,\frac{\gamma(\beta^2 z - \beta c t)}{b+a}. \tag{3}$$

This yields the potentials

$$\Phi = -\frac{\gamma Z e}{\sqrt{(x-b)^2 + y^2 + d^2 + \gamma^2(z-\beta c t)^2}} + \frac{\gamma Z e}{\sqrt{(a+b)^2 + \gamma^2(\beta^2 z - \beta c t)^2}}, \tag{4a}$$

$$A_x = 0, \tag{4b}$$

$$A_y = 0, \tag{4c}$$

$$A_z = \beta\Phi, \tag{4d}$$

which fall off as z^{-2}, sufficiently fast for a stable numerical treatment. The gauge parameter a is chosen to coincide with the cutoff parameter d.

C. Propagation and observables

Initially the target is in its ground state $|\Psi_0\rangle$ with the projectile infinitely remote (in practice, far enough away to have no effect). Let us associate with that the state $|\Psi(-T)\rangle = |\Psi_0\rangle$ where we think ideally $T\rightarrow\infty$. From that starting point, we propagate the electronic state $|\Psi(t)\rangle$ by TDDFT under the influence of the external potentials (4). We solve the TDDFT equations for the single-electron wave functions φ_α from which $|\Psi(t)\rangle$ is composed on a grid in three-dimensional coordinate space; for details, see Refs. [21,22]. At the end, we can compute the total inelastic transition probability η for one specific scattering event as

$$\eta(\beta,b;\theta,\phi) = \lim_{T\rightarrow+\infty}\left[1 - |\langle\Psi_0|\Psi(T)\rangle|^2\right]. \tag{5a}$$

The probability η depends on the ionic velocity β, impact parameter b, and the initial molecular orientation θ,ϕ. This orientation is meaningless for atoms that are spherical. Two angles suffice to determine axially symmetric molecules. One would need three Euler angles when considering triaxial molecules (which is not done here). The total inelastic transition cross section σ is obtained from integrating η over all impact parameters with equal weight (homogeneous flow) and, if necessary, averaging over all molecular orientations, i.e.,

$$\sigma(\beta) = \frac{1}{4\pi^2}\int_0^{2\pi} d\phi \int_0^{\pi} d(\cos\theta) \int_0^{\infty} db\, b\,\eta(\beta,b;\theta,\phi). \tag{5b}$$

Thus far, the concept is straightforward. But it turns out that it becomes impracticable in many situations. The reason is that the external field can cover any time scale depending on the impact parameter b. For $b \approx 1a_0$ being of atomic scale (where a_0 is the Bohr radius), the external pulse varies at the rate of attoseconds. A detailed time propagation becomes extremely expensive because it has to resolve that scale while substantial changes at the atomic site take several femtoseconds (fs) to develop. On the other hand, the external pulse becomes long and slow for very large impact parameters while the atomic scale with its typical cycle of fs remains fully resolved. It is obvious that we have to cope with very different dynamical regimes. To this end, we develop a particularly suited approximation for each regime separately. We will check these approaches by comparison with the exact propagation and we will work out an appropriate switching point between the regimes.

D. Approaches

1. The sudden approximation

In the limit of extremely fast excitation, the external perturbation

$$\hat{V}(t) = e\Phi + \frac{e}{c}(\hat{\mathbf{p}}\cdot\mathbf{A} + \mathbf{A}\cdot\hat{\mathbf{p}}) \tag{6}$$

is concentrated on a very short instant around $t=0$. The electronic dynamics is practically frozen while the external field passes by. Its only effect is to modify “at once” the phase of the electronic wave functions. The phase pattern thus imprinted determines the further evolution. The concept is very similar to the Glauber approximation often used in scattering theory [18,19]. The adaption of Glauber theory for the present case of sudden Coulomb excitation was studied extensively in Ref. [24]. The basic steps are summarized in Appendix A. It turns out that the accumulated phase profile becomes

$$\hat{S} = \sum_{i=1}^{N}\frac{Ze^2}{\beta c}\ln[(x_i-b)^2 + y_i^2 + d^2], \tag{7a}$$

and with it the total inelastic transition probability

$$\eta = 1 - |\langle\Psi_0|e^{-\imath\hat{S}}|\Psi_0\rangle|^2. \tag{7b}$$

The propagation in the regime $t>0$ after excitation does not change the distribution of excited states. The probability can thus be read off immediately after excitation. The criterion for the validity of the sudden approximation is

$$\frac{2b}{\gamma\beta c} \ll \frac{1}{E_{\mathrm{exc}}}, \tag{8}$$

where E_{exc} is the lowest excitation energy in the system. Such conditions are only a rough guideline. We will check the range of validity in practice later.

The total inelastic transition probability (7) is particularly simple to evaluate because only the ground state is involved. With a bit more effort, one can also compute excitation probabilities for specific states $|\Psi_\alpha\rangle$ in the sudden approximation. These read

$$\eta_{0\alpha} = |\langle\Psi_\alpha|e^{-\imath\hat{S}}|\Psi_0\rangle|^2. \tag{9}$$

We will use that possibility to elucidate in the following studies the various contributions to the total cross section.

2. Perturbation theory

The other extreme is the weak and slow fields that emerge in the case of very large impact parameters b. The magnetic field becomes negligible and the electrical field at the target site can be treated in dipole approximation. There remains the perturbation Hamiltonian

$$\hat{V} = -\mathbf{E}_0(t)\cdot\hat{\mathbf{D}}, \tag{10a}$$

$$E_{0x}(t) = \frac{\gamma Zeb}{[b^2+d^2+\gamma^2\beta^2c^2t^2]^{3/2}}, \tag{10b}$$

$$E_{0y}(t) = 0, \tag{10c}$$

$$E_{0z}(t) = \frac{-\gamma\beta ctZe}{[b^2+d^2+\gamma^2\beta^2c^2t^2]^{3/2}}, \tag{10d}$$

where $\hat{\mathbf{D}}$ is the dipole operator and $\mathbf{E}_0$ the electrical field at the origin. The details of time-dependent perturbation theory and subsequent approximations are given in Appendix B. From that, we can deduce upper and lower limits for the total inelastic transition probabilities in the regime of remote collisions,

$$\eta_{\max} = \frac{4(Ze)^2}{\beta^2c^2b^2}\Omega_{10}K_1^2(\Omega_{10})\langle\Psi_0|\Delta^2\hat{D}_x|\Psi_0\rangle, \tag{11a}$$

$$\eta_{\min} = \frac{4(Ze)^2}{\beta^2c^2b^2}\Omega_{10}K_1^2(\Omega_{10})|D_{x,10}|^2, \tag{11b}$$

$$\Omega_{10} = \left(\frac{b\omega_{10}}{\gamma\beta c}\right), \tag{11c}$$

where $\Delta\hat{D}_x=\hat{D}_x-\langle\Psi_0|\hat{D}_x|\Psi_0\rangle$, $D_{x,10}=\langle\Psi_1|\hat{D}_x|\Psi_0\rangle$, and $\hat{D}_x$ is the operator of the dipole in the x direction. The K_1 is a modified Bessel function. This function decays exponentially and thus the excitation probabilities fall off exponentially with the impact parameter b rendering the total transition cross section finite. The upper and lower limits converge toward each other in the limit of large impact parameters b. We will use the upper limit as a reliable estimate for the total inelastic transition probability, i.e., $\eta \approx \eta_{\max}$.

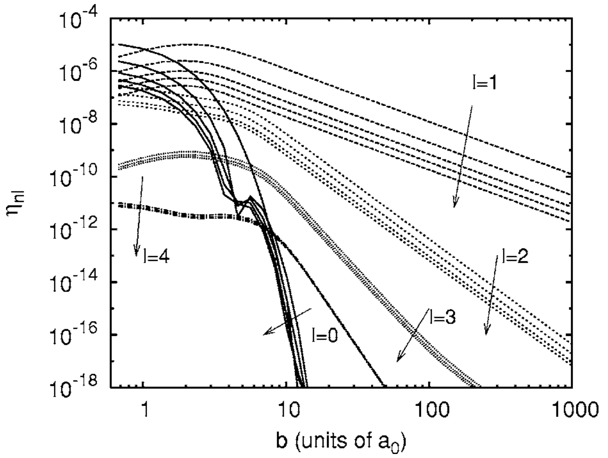

FIG. 1. Detailed excitation probabilities η_{nl} for excitation of a hydrogen atom by a fast proton with velocity $\beta=v/c=0.99$ at various impact parameters b. We show specific transitions from the 1s state to the various excited states nl in the hydrogen atom computed in sudden approximation. The results gather in bunches of same angular momentum l and different n. The groups are indicated by embracing arrows labeled with the corresponding l.

There is an intermediate range of impact parameters b where the dipole approximation for the spatial part of the excitation operator becomes valid while the sudden approximation is still at work concerning the temporal profile. This is a regime where both approximations nicely match. Thus we do not need the explicitly time-dependent calculations except for critical tests of either approximation.

3. Consequences for practical calculations

Both, the sudden approximation and perturbative estimates yield formulas that involve merely stationary states. That is a great simplification because these are much faster to compute than a full time evolution. Moreover, we can exploit spherical symmetry in the case of atoms. We take advantage of that simplification for most of the detailed studies concerning the distribution of excitation channels. The final results for the total ionization cross sections for all systems, atoms and molecules, are done on the basis of a fully three-dimensional code.

III. RESULTS AND DISCUSSION

A. Disentangling the contributions: Hydrogen

In this section, we are going to study the various contributions to the excitations in detail. To that end, we compute the detailed transition probabilities in sudden approximation according to Eq. (9). As a simple test case we consider scattering of a fast proton by a hydrogen atom as target. Figure 1 shows the distribution of transition probabilities for hydrogen as a function of the impact parameter. The monopole ($l=0$) dominates for small impact parameters $b<1a_0$. The dipole ($l=1$) dominates everywhere else and thus will contribute dominantly to the total cross section. Contributions from higher angular momenta l decrease quickly with increasing l. Moreover, the fall off with b becomes faster with

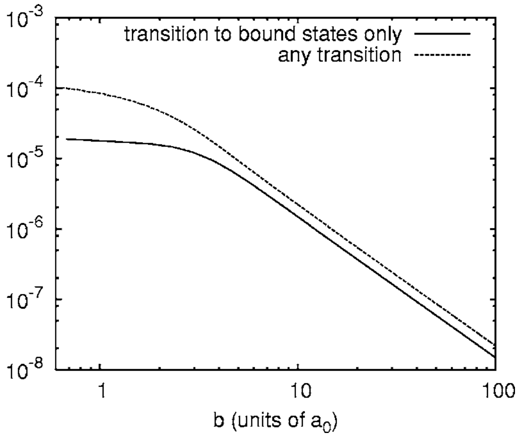

FIG. 2. Total inelastic transition probability η (dashed) and sum of excitations to bound states only (solid) for excitation of a hydrogen atom by a fast proton with velocity $\beta = v/c = 0.99$ at various impact parameters b.

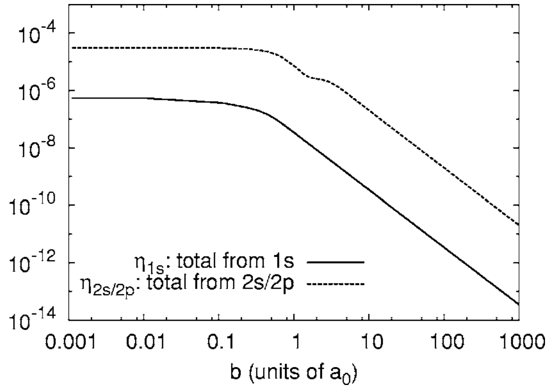

FIG. 3. Probabilities for excitation of a Ne atom by a fast proton with velocity $\beta = v/c = 0.99$ at various impact parameters b. We show the probability for excitations from the valence $2s$-$2p$ shell (dashed) and from the deep lying $1s$-core state (solid).

increasing l. This trend starts rather early. Note, however, that the regime of large $b > 100a_0$ lies outside the range of validity of the sudden approximation. There, all excitation probabilities fall off faster (namely exponential), see Eq. (11), than the results of the sudden approximation (power laws of order increasing with l).

A basic distinction in the excitation spectrum exists between bound states and the particle continuum. In Fig. 2, the total inelastic transition probability is compared with the excitation to bound states, again for the test cases of hydrogen. The difference is then the ionization probability. For small b, ionization processes prevail. Their contribution decreases with increasing b remaining about 30% in an intermediate range, in agreement with previous studies [25,26]. The trend is obviously related to the time scale of the excitation in dependence of the impact parameter. Small b means very fast collisions. These carry a great deal of high frequencies thus spreading the excitations broadly over the spectrum. The temporal profile grows broader with increasing b. This depletes gradually the high frequencies and gives more weight to the low-energy excitation which resides naturally in the realm of bound states. Eventually, only the lowest dipole transition remains. But such slow processes emerge only for large b far outside the scale shown in the figure.

B. Disentangling the contributions: Atoms

Many-electron atoms display a much richer spectrum than hydrogen. Excitations differ not only by the excited levels reached but also by the originally occupied levels from which the electron is removed. The electronic states in an atom are sorted into core states of different depth and finally the valence shell which is least bound. The energetic differences in binding are dramatic with the valence states typically bound by about 5 eV while core states range at the order of 100 eV and more of binding. One expects intuitively that the valence shell dominates in the excitation processes. This conjecture is checked in Fig. 3 showing separately the excitation from valence and core states of the Ne atom. The result proves nicely that core states can indeed be neglected in computing the total inelastic transition probabilities. This is what we will adopt in the following.

Figure 4 shows the total inelastic transition probabilities for a few typical atoms. As worked out in the previous test case, the excitations are taken as outgoing from the valence shell only. Pattern and order of magnitude are very similar. There is a systematic shift of the peak position with impact parameter. The effect is obvious. The rare gas Ne is deepest bound and has the smallest radius. Binding is weakened when removing one electron after another. The increasing peak impact parameter will lead to increasing cross sections, although the peak height is almost the same in all cases. Nonetheless, the effects remain moderate and we will find all cross sections stay at the same order of magnitude.

C. Angular averaging

Molecules are nonspherical objects. Thus we have as an additional degree of freedom the orientation of the molecule relative to the impinging fast ion. The effect of relative ori-

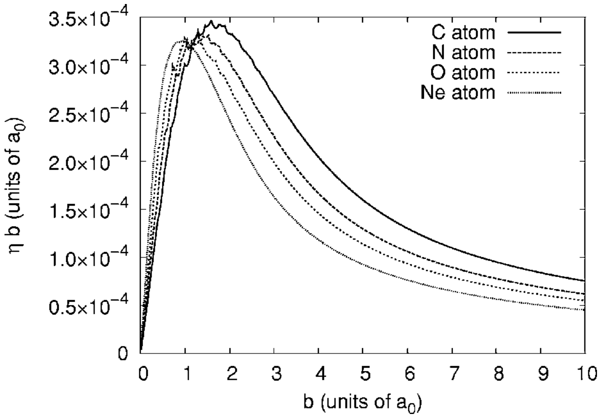

FIG. 4. Total inelastic transition probabilities for transitions from the ground state of different atoms (as indicated) by a fast proton with velocity $\beta = v/c = 0.99$ at various impact parameters b computed with the sudden approximation.

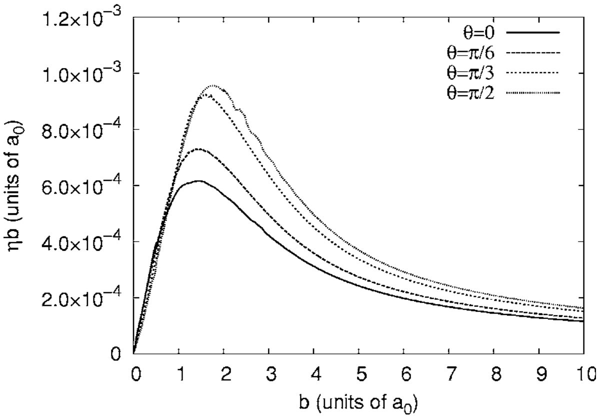

FIG. 5. Total inelastic transition probability for the collision of velocity $\beta = v/c = 0.99$ with a N_2 molecule as function of the impact parameter b. Results are shown for various orientations of the molecular axis with respect to the z axis (= direction of propagation of the proton). All results are obtained with the sudden approximation.

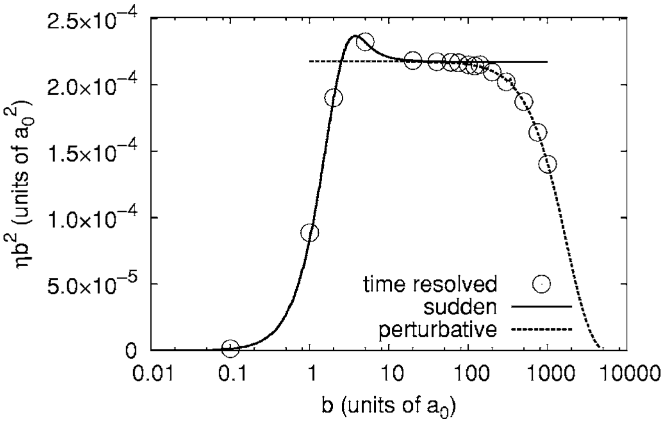

FIG. 6. Total inelastic transition probability for the proton-hydrogen collision with proton velocity $\beta = v/c = 0.99$ as a function of the impact parameter b. Results from various approximations are compared as indicated. The probabilities are scaled by b^2 to display them relative to the asymptotics of the sudden approximation.

entation is shown in Fig. 5 for the case of a N_2 molecule. There are visible differences. Thus one needs to perform a set of calculations at a bunch of different orientations and to average the cross section over these orientations. However, the results do not vary too much and stay all nicely within the same order of magnitude. This allows us to use only a coarse grid in the space of orientations. Actually, we will take a step of $\pi/24$ radians for each Euler angle. Of course, one can make use of symmetry and confine calculations of cylindrical molecules to the interval $[0,\pi]$ for θ or even $[0,\pi/2]$ for dimers like N_2.

D. Matching the regimes

In all the above explorations, we have considered the sudden approximation throughout. This approach must fail for large impact parameters where the transition probabilities fall off too slowly as b^{-2} yielding infinite cross sections. Connecting to the perturbative regime for large b is compulsory in order to generate the correct asymptotics of the transition probabilities. The analytical studies indicate that the sudden approximation and the perturbation theory have a common regime of validity. We check that in Fig. 6 by comparison with the fully time-resolved calculations. Both approaches agree very nicely with the exact results in their regime of validity, which is $b < 100a_0$ for the sudden approximation and $b > 100a_0$ for the perturbative estimate. There is also a sufficiently large range of common validity around $b \approx 100a_0$. Figure 6 suggests the following procedure: We compute the sudden approximation as well as the perturbative estimate over a broad range of b. We switch in the center of the b interval where both approaches match. This yields a reliable estimate for the total inelastic transition probability for all b, which then is finally integrated to obtain the total transition cross section.

E. Total cross sections

We have developed a well defined procedure to compute total inelastic transition cross sections for atoms and molecules when colliding with a fast ion. A summary of results for a broad range of ionic velocities is shown in Fig. 7 for a variety of atoms and molecules. The velocity is shown in terms of γ in order to provide a convenient scale for the plot. Large γ correspond to large velocities and energies. For example, in the case of a proton beam, $\gamma = 50$ equals an energy of 46.9 GeV per proton. All cross sections display the same trends with a minimum at around $\gamma \approx 3.7$, which corresponds to 3.5 GeV and a slow but steady increase with γ.

The similarity of the cross sections suggests that the leading difference is caused by a trivial factor. The dominance of the dipole contribution found in Sec. III A and the expressions worked out in Sec. II suggest that this factor is related to the dipole matrix elements. We thus try to extract the dipole variance $\Delta^2 D = \langle \Psi_0 | \Delta^2 \hat{D}_x | \Psi_0 \rangle$ by rescaling the cross sections relative to the dipole variance of the hydrogen atom. The result is shown in Fig. 8. The rescaling compresses indeed all cross sections into a narrowband of about 5% width. This means at the end that all transition cross sections can be estimated in a rather simple manner by computing just the dipole variance for the ground state of the atom or molecule

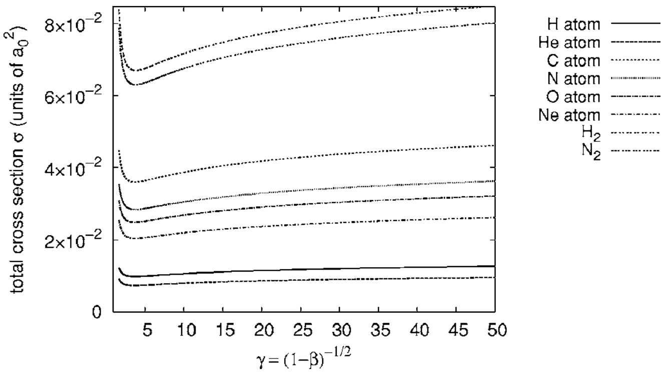

FIG. 7. Total inelastic transition cross sections for the collision of fast protons with atoms and molecules. The cross sections are shown as function of ionic γ for a selection of typical atoms and molecules.

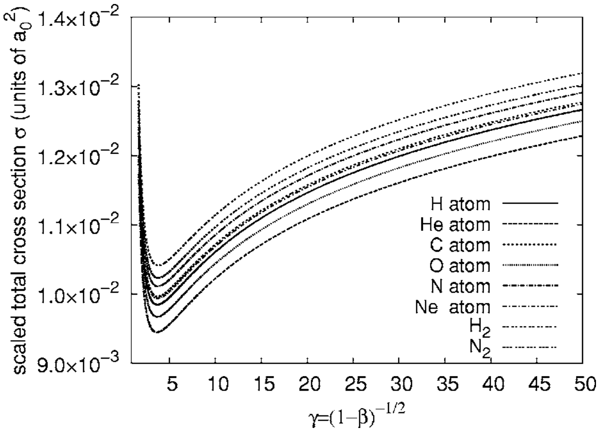

FIG. 8. Total inelastic transition cross sections as in Fig. 7 but scaled by the relative dipole variances $\Delta^2 D_{\mathrm{H}}/\Delta^2 D_X$, where H stands for hydrogen and X for the actual atom or molecule.

of interest and multiplying that with the well known cross section of the hydrogen atom, which is given by Eq. (B6).

The dipole variances have yet to be calculated in detail, e.g., by a DFT code. The question arises whether one can derive a simple systematics for that piece of information. Figure 9 shows the dipole variance for the systems under consideration. There is some regularity to the extent that the atoms can be sorted nicely according to groups of elements and that the dimers belong visibly to a much different category. However, a simple estimate covering all systems is not immediately obvious and may become hopeless when extending the class of molecules under consideration. It is probably not worth the effort in view of the fact that (merely static) DFT calculations are readily available.

One can, however, simplify the other entry in the estimate, the cross section for hydrogen as given in Eq. (B6). By expanding the Bessel functions for small arguments up to first order, we obtain

$$\frac{\sigma_H(\beta)}{a_0^2} \approx \frac{Z^2}{\beta^2}\{5.287 \times 10^{-3} + \pi 6.695 \times 10^{-4}[-2.4037 + 2\ln(\gamma\beta)]\}, \qquad (12)$$

which turns out to provide a surprisingly good approximation. In the SIS100 storage ring at the GSI Darmstadt (for parameters, see Refs. [23]) with a beam energy of up to 29 GeV/u for the approximately 10^{13} protons which move in a tube of a circumference of 1083.6 m containing an estimated residual gas density of about $n_g = 10^{11}\ \mathrm{m}^{-3}$, this would yield a transition rate of about $\tau^{-1} = 10^{10}\ \mathrm{s}^{-1}$ for the case of a residual gas consisting of hydrogen atoms only.

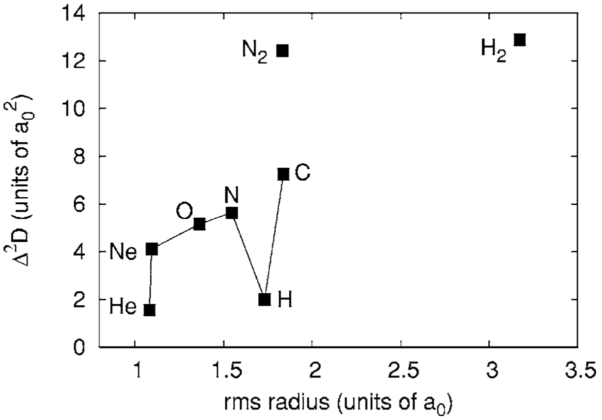

FIG. 9. The angular averaged dipole sum G over the rms radius of the electron density for different systems under study.

IV. CONCLUSIONS

We have investigated the transitions of atoms and small molecules from their ground state through collisions with highly relativistic charged ions. The ion was assumed to travel unperturbed on a straight trajectory acting on the target by delivering an electromagnetic force pulse. We have performed fully time-resolved calculations using the time-dependent Schrödinger equation for the hydrogen atom or time-dependent density-functional theory for many-electron systems. This serves for principal investigations and for testing the various approximations.

Close collisions with impact parameters $b \lesssim 100 a_0$ are related to extremely short force pulses. These can be approximated very well in a sudden approximation where the change in the local momentum is imprinted instantaneously on the electron cloud as a modification of its phase profile. This defines at once the distribution of excitation energy over the spectrum of excited states. The detailed time evolution starts from this (instantaneously excited) initial state where the consequences of the excitation profile are becoming manifest in the course of time. The excitation (and ionization) probability can be evaluated simply from the initial state in comparison to the unperturbed spectrum.

Distant collisions produce more slowly changing fields at the target site which cannot be treated in sudden approximation. On the other hand, such fields are very weak and can be treated very well by time-dependent perturbation theory. Fortunately, the regimes of validity of both approximations have a large overlap such that both approaches complement each other nicely. We combine them with an appropriate switching impact parameter in the center of the overlap regime. The simplified treatment thus derived has been counterchecked by the full-fledged time-dependent calculations.

The remaining expressions and matrix elements can still be rather lengthy and hard to calculate for many-electron systems. Using all-electron calculations, we have shown that by far the dominant contribution to the excitation and ionization probabilities comes from the valence shell. All deeper-lying core states need not be treated explicitly and can be replaced by pseudopotentials.

Taking these three approximations together, we need only a few static density-functional calculations for the valence states of a system to compute the transition cross sections. We have considered in detail the cross sections for H, He, C, N, O, Ne, H_2, and N_2. From the systematics of the results thus obtained, we find that an even simpler estimate is possible. The cross section for a given target system separates into the generic cross section of hydrogen atom times the variance of the dipole operator for the valence shell of the given system. The hydrogen cross section carries all velocity dependence while the dipole variance serves as a scale factor.[28–38]

ACKNOWLEDGMENTS

This work was supported by the German Ministry for Education and Research, project number BMBF 06 ER 128.

APPENDIX A: DETAILS OF THE SUDDEN APPROXIMATION

The time evolution operator in the interaction picture reads

$$|\Phi(t)\rangle_I = \hat{U}(t,t_0)|\Phi(t_0)_I, \tag{A1a}$$

$$\hat{U}(t,t_0) = \sum_{n=0}^{\infty} \frac{(-i)^n}{n!} \mathcal{T}\left[\int_{t_0}^{t} dt' \{V_I(t')\} \right]^n, \tag{A1b}$$

$$V_{\mathrm{I}}(t') = e^{i\hat{H}_0(t'+T)} \hat{V}_S(t') e^{-i\hat{H}_0(t'+T)}, \tag{A1c}$$

where

$$\mathcal{T}[A(t),B(t')] = \begin{cases} A(t)B(t') & \text{for } t \geqslant t' \\ B(t')A(t) & \text{for } t < t' \end{cases} \tag{A1d}$$

is the time-ordering operator and $\hat{V}_S$ describes the time-dependent external perturbation. The index I denotes a state vector or operator in the interaction picture and S in the Schrödinger picture. We are now considering close collisions where the potential V_S has nonvanishing values only in a very small vicinity of $t=0$. In that case, the time ordering operator can be ignored, the whole excitation shrinks to an instantaneous process, and the dynamics proceeds in three regimes as

$$t < 0^-: \quad |\Psi(t) = e^{-iE_0 t}|\Psi_0\rangle,$$

$$0^- < t < 0^+: \quad |\Psi(0^+) = e^{-i\int_{-\infty}^{\infty} dt' \, \hat{V}_S(t')}|\Psi(0^-)\rangle,$$

$$0^+ < t: \quad |\Psi(t) = e^{-i\hat{H}_0 t}|\Psi(0^+)\rangle, \tag{A2}$$

where $0^{\pm}=0\pm\epsilon$ stands for instant short before and after excitation. The further propagation $e^{-i\hat{H}_0 t}$ does not change the internal structure of the state. The amount of excitation is determined at the instant of excitation and we obtain the total inelastic transition probability as

$$\eta = 1 - |\langle\Psi_0|\hat{U}_{\mathrm{sudden}}|\Psi_0|\rangle|^2,$$

$$\hat{U}_{\mathrm{sudden}} = \exp\left(-i \int_{-\infty}^{\infty} dt' \, \hat{V}_S(t') \right). \tag{A3}$$

Using the explicit perturbation (6) with the potentials (4), we obtain

$$\hat{S} = \int_{-\infty}^{\infty} dt' \, \hat{V}_S(t') = \sum_{i=1}^{N} \frac{Ze^2}{\beta c} \ln[(x_i - b)^2 + y_i^2 + d^2]. \tag{A4}$$

We can neglect the vector potential terms here because it only enters the z component of the electric field, which is an odd function of time. In sudden approximation, the perturbation is integrated over all time such that its z component does not contribute to the excitation process [24].

APPENDIX B: DETAILS OF THE PERTURBATION THEORY

Starting from the perturbation (10), we obtain by standard time-dependent perturbation theory the excitation probability,

$$\begin{aligned} \eta(b) &= \frac{4(Ze)^2}{\beta^2 c^2} \frac{1}{b^2} \sum\!\!\!\!\!\!\!\int_{\alpha\neq 0} \left[\left| D_{x,\alpha 0} \right|^2 \Omega^2 K_1^2(\Omega) \right. \\ &\quad \left. + \frac{1}{\gamma^2} |D_{z,\alpha 0}|^2 \Omega_{\alpha 0}^2 K_0^2(\Omega_{\alpha 0}) \right] \\ &\approx \frac{4(Ze)^2}{\beta^2 c^2} \frac{1}{b^2} \sum\!\!\!\!\!\!\!\int_{\alpha\neq 0} D_{x,\alpha 0}^2 \Omega_{\alpha 0}^2 K_1^2(\Omega_{\alpha 0}), \end{aligned} \tag{B1}$$

$$\Omega_{\alpha 0} = \frac{b\omega_{\alpha 0}}{\gamma\beta c}, \tag{B2}$$

$$\sum\!\!\!\!\!\!\!\int_{\alpha\neq 0} = \sum_{\alpha\neq 0 \in \mathrm{discrete}} + \int_{\alpha \in \mathrm{continuum}} d\alpha, \tag{B3}$$

where K_i is a modified Bessel function of the second kind [27]. One can neglect the second term because of the factor γ^{-2} and because for small arguments x: $K_1(x) \gg K_0(x)$.

The summation over all discrete excited states and subsequent integration over all continuum states is, of course, a cumbersome operation. As a further step, we derive an approximation and upper bound. Using

$$x' > x \Rightarrow x'^2 K_1^2(x') < x^2 K_1^2(x),$$

we obtain

$$\eta \leqslant \eta_{\max} = \frac{4(Ze)^2}{\beta^2 c^2} \frac{1}{b^2} G \Omega_{10}^2 K_1^2(\Omega_{10}), \tag{B4a}$$

$$G = \sum\!\!\!\!\!\!\!\int_{\alpha\neq 0} |\langle\Psi_\alpha|D_x|\Psi_0\rangle|^2 = \langle\Psi_0|\Delta^2 D_x|\Psi_0\rangle, \tag{B4b}$$

$$\Delta D = \hat{D}_x - \langle\Psi_0|\hat{D}_x|\Psi_0\rangle. \tag{B4c}$$

It is equally simple to deduce a lower estimate. One simply restricts the summation to the lowest excitations and obtains

$$\eta \geqslant \eta_{\min} = \frac{4(Ze)^2}{\beta^2 c^2} \frac{1}{b^2} \Omega_{10}^2 K_1^2(\Omega_{10}) |D_{x,10}|^2. \tag{B5}$$

The expression is very similar to the upper estimate (B4a). The difference consists only in the range of the dipole sum, full variance versus lowest excitation only. The external field becomes ever slower with increasing impact parameter b. This puts increasing weight on the lowest (=slowest) excitation. In the limit $b \rightarrow \infty$, the true perturbative excitation probability approaches this lower bound so that Eq. (B4a) is an overestimation. However, such extremely large collision parameters do not contribute significantly to the total cross section. As a result, the error by using Eq. (B4a) is negligible.

Using Eq. (B4a), one can easily integrate the perturbative part of the cross section analytically. Before doing so, in the case of molecules we have to average over all orientations of the molecular axis relative to the projectile trajectory. In the perturbative expression, this can be done by substituting $G = \langle \Psi_0 | \Delta^2 D_x | \Psi_0 \rangle \rightarrow \langle \Psi_0 | \Delta^2 \mathbf{D} \cdot \mathbf{n}(\theta, \phi) | \Psi_0 \rangle$, and averaging over the Euler angles θ and ϕ. This is also an easy operation since only the stationary ground-state wave function is involved. After integrating, we finally get for the cross section as a function of the velocity $\beta = v/c$

$$\sigma = 2\pi \int_0^{b_1} db\, b\, \eta_{\text{sudden}} + \pi G \frac{4(Ze)^2}{\beta^2 c^2} \Omega_{10}^2 \times [K_0(\Omega_{10}) K_2(\Omega_{10}) - K_1^2(\Omega_{10})], \tag{B6}$$

where G was given in Eq. (B4b), $\Omega_{10} = b_1 \omega_{10} / \gamma\beta c$, and b_1 is the switching point between sudden approximation and treatment in perturbation theory.

[1] J. Eichler and W. E. Meyerhof, *Relativistic Atomic Collisions* (Academic, New York, 1995).
[2] H. Bethe, Ann. Phys. **5**, 325 (1930).
[3] S. P. Slinker, R. D. Taylor, and A. W. Ali, J. Appl. Phys. **63**, 1 (1988).
[4] M. E. Rudd, Y.-K. Kim, D. H. Madison, and J. W. Gallagher, Rev. Mod. Phys. **57**, 965 (1985).
[5] J. H. Scofield, Phys. Rev. A **18**, 963 (1978).
[6] D. M. Davidovic, B. L. Moiseiwitsch, and P. H. Norrington, J. Phys. B **11**, 847 (1978).
[7] R. Anholt, Phys. Rev. A **19**, 1004 (1979).
[8] R. Anholt, W. E. Meyerhof, H. Bowman, and D. H. H. Hoffmann, Phys. Rev. A **30**, 2234 (1984).
[9] T. Ludziejewski, Th. Stöhlker, D. C. Ionescu, P. Rymuza, H. Beyer, F. Bosch, C. Kozhuharov, K. Krämer, D. Liesen, P. H. Mokler, Z. Stachura, P. Swiat, A. Warczak, and R. W. Dunford, Phys. Rev. A **61**, 052706 (2000).
[10] D. Madison, M. Schulz, S. Jones, M. Foster, R. Moshammer, and J. Ullrich, J. Phys. B **35**, 3297 (2002).
[11] O. Busic, N. Grün, and W. Scheid, Phys. Rev. A **70**, 062707 (2004).
[12] A. B. Voitkiv, B. Najjari, and J. Ullrich, Phys. Rev. Lett. **92**, 213202 (2004).
[13] A. B. Voitkiv, B. Najjari, and J. Ullrich, Phys. Rev. Lett. **94**, 163203 (2005).
[14] M. T. F. Pivi and M. A. Furmann, Phys. Rev. ST Accel. Beams **6**, 034201 (2003).
[15] M. Blaskiewicz, M. A. Furman, M. Pivi, and R. J. Macek, Phys. Rev. ST Accel. Beams **6**, 014203 (2003).
[16] J. Bosser (private communication).
[17] E. K. U. Gross, J. F. Dobson, and M. Petersilka, Top. Curr. Chem. **181**, 81 (1996).
[18] V. Franco, Phys. Rev. Lett. **20**, 709 (1968).
[19] V. Franco and B. K. Thomas, Phys. Rev. A **4**, 945 (1971).
[20] D. Dimitrovski, E. A. Solov'ev, and J. S. Briggs, Phys. Rev. Lett. **93**, 083003 (2004).
[21] F. Calvayrac, P.-G. Reinhard, E. Suraud, and C. Ullrich, Phys. Rep. **337**, 493 (2000).
[22] P.-G. Reinhard and E. Suraud, *Introduction to Cluster Dynamics* (Wiley, Berlin, 2003).
[23] Gesellschaft für Schwerionenforschung (GSI), *An International Accelerator Facility for Beams of Ions and Antiprotons – Conceptual Design Report*, Darmstadt, 2001.
[24] B. Jakob, Diploma thesis, University of Erlangen (2002).
[25] J. Marten and C. Toepffer, Eur. Phys. J. D **29**, 397 (2004).
[26] J. Marten, Dissertation, University of Erlangen (2003).
[27] M. Abramowitz and I. Stegun, *Handbook of Mathematical Functions* (Dover Publications, New York, 1964).
[28] M. Bär, Diploma thesis, University of Erlangen (2005).
[29] D. Dimitrovski, T. P. Grozdanov, E. A. Solov'ev, and J. S. Briggs, J. Phys. B **36**, 1351 (2003).
[30] U. Becker, N. Grün, and W. Scheid, J. Phys. B **18**, 4589 (1985).
[31] P. A. Amundsen and K. Aashamar, J. Phys. B **14**, 4047 (1981).
[32] F. F. Rieke and W. Prepejchal, Phys. Rev. A **6**, 1507 (1972).
[33] M. Reiser, *Theory and Design of Charged Particle Beams* (J. Wiley & Sons, New York, 1994).
[34] A. B. Voitkiv, J. Phys. B **38**, 1773 (2005).
[35] R. Moshammer, J. Ullrich, M. Unverzagt, W. Schmitt, P. Jardin, R. E. Olson, R. Mann, R. Dörner, V. Mergel, U. Buck, and H. Schmidt-Böcking, Phys. Rev. Lett. **73**, 3371 (1994).
[36] M. Schulz, R. Moshammer, D. H. Madison, R. E. Olson, P. Marchalant, C. T. Whelan, H. R. J. Walters, S. Jones, M. Foster, H. Kollmus, A. Cassimi, and J. Ullrich, J. Phys. B **34**, L305 (2001).
[37] P. D. Fainstein, V. H. Ponce, and R. D. Rivarola, J. Phys. B **24**, 3091 (1991).
[38] D.-C. Ionescu and Th. Stöhlker, Phys. Rev. A **67**, 022705 (2003).